

UC Berkeley

UC Berkeley Previously Published Works

Title

para-Aminobenzoic Acid Biosynthesis Is Required for *Listeria monocytogenes* Growth and Pathogenesis

Permalink

<https://escholarship.org/uc/item/6tq8j3f3>

Journal

Infection and Immunity, 90(11)

ISSN

0019-9567

Authors

Zhang, Yingying

Anaya-Sanchez, Andrea

Portnoy, Daniel A

Publication Date

2022-11-17

DOI

10.1128/iai.00207-22

Peer reviewed



para-Aminobenzoic Acid Biosynthesis Is Required for *Listeria monocytogenes* Growth and Pathogenesis

Yingying Zhang,^{a,b*} Andrea Anaya-Sanchez,^c  Daniel A. Portnoy^{a,d}

^aDepartment of Molecular and Cell Biology, University of California, Berkeley, Berkeley, California, USA

^bCalifornia Institute for Quantitative Biosciences-Berkeley (QB3-Berkeley), University of California, Berkeley, Berkeley, California, USA

^cGraduate Group in Microbiology, University of California, Berkeley, Berkeley, California, USA

^dDepartment of Plant and Microbial Biology, University of California, Berkeley, Berkeley, California, USA

ABSTRACT Biosyntheses of *para*-aminobenzoic acid (PABA) and its downstream folic acid metabolites are essential for one-carbon metabolism in all life forms and the targets of sulfonamide and trimethoprim antibiotics. In this study, we identified and characterized two genes (*pabA* and *pabBC*) required for PABA biosynthesis in *Listeria monocytogenes*. Mutants in PABA biosynthesis were able to grow normally in rich media but not in defined media lacking PABA, but growth was restored by the addition of PABA or its downstream metabolites. PABA biosynthesis mutants were attenuated for intracellular growth in bone marrow-derived macrophages, produced extremely small plaques in fibroblast monolayers, and were highly attenuated for virulence in mice. PABA biosynthesis genes were upregulated upon infection and induced during growth in broth in a strain in which the master virulence regulator, PrfA, was genetically locked in its active state (PrfA*). To gain further insight into why PABA mutants were so attenuated, we screened for transposon-induced suppressor mutations that formed larger plaques. Suppressor mutants in *relA*, which are predicted to have higher levels of (p)ppGpp, and mutants in *codY*, which is a GTP-binding repressor of many biosynthetic genes, partially rescued the plaque defect but, notably, restored the capacity of the mutants to escape from phagosomes and induce the polymerization of host cell actin. However, these suppressor mutant strains remained attenuated for virulence in mice. These data suggest that even though folic acid metabolites exist in host cells and might be available during infection, *de novo* synthesis of PABA is required for *L. monocytogenes* pathogenesis.

KEYWORDS *Listeria monocytogenes*, PABA, *para*-aminobenzoic acid, folic acid, pathogenesis

Listeria monocytogenes is a Gram-positive bacterium that lives a biphasic life as a saprophyte and as a facultative intracellular pathogen of animals and humans. This opportunistic pathogen infects humans through consumption of contaminated food and can cause severe diseases in pregnant women, neonates, the elderly, and immunocompromised individuals. The clinical manifestations of listeriosis range from self-limiting enteritis to life-threatening sepsis, meningoenzephalitis, and miscarriage (1, 2).

Upon infection, multiple *L. monocytogenes* virulence factors function together to orchestrate the tightly regulated infection process leading to successful entry, phagosomal escape, rapid replication, actin-based movement, and spread from cell to cell (3). The pore-forming cytolysin, listeriolysin O (LLO; encoded by the gene *hly*), is required for phagosomal escape, and the ActA surface protein is necessary for actin-based motility and cell-to-cell spread (4, 5). Many of the known virulence genes reside in the PrfA regulon. PrfA is the master transcription activator which is regulated at multiple levels to achieve full activity during intracellular growth and is allosterically regulated by glutathione (GSH) produced by the *L. monocytogenes* glutathione synthase (GshF) (6, 7). However, the requirement for

Editor Sabine Ehrt, Weill Cornell Medical College

Copyright © 2022 American Society for Microbiology. All Rights Reserved.

Address correspondence to Daniel A. Portnoy, portnoy@berkeley.edu.

*Present address: Yingying Zhang, State Key Laboratory of Cellular Stress Biology, Innovation Center for Cell Biology, School of Life Sciences, Xiamen University, Xiamen, Fujian, China.

The authors declare no conflict of interest.

Received 18 May 2022

Returned for modification 13 June 2022

Accepted 23 September 2022

Published 1 November 2022

GSH can be bypassed by a mutation in PrfA that locks the protein in its active conformation; this protein is referred to as PrfA* (6).

L. monocytogenes has relatively few growth requirements, although it does require some B vitamins that it obtains from its host, including riboflavin, thiamine, biotin, and lipoic acid. Starvation for riboflavin or lipoic acid results in bacteria that are unable to grow in cells (8). Like most bacteria, fungi, and plants, but not mammals, *L. monocytogenes* can synthesize folic acid (FA) and its metabolites by first synthesizing its precursor *para*-aminobenzoic acid (PABA). Folic acid is required for one-carbon metabolism in all forms of life for the formation of purines, pyrimidines, formyl-methionyl tRNA^{fMet}, thymidine, serine, methionine, and glycine (9, 10). Since humans are unable to synthesize folates and most bacteria are unable to transport folic acid or its metabolites, antibiotics that target folic acid biosynthesis are highly effective against many bacterial pathogens, including *L. monocytogenes* (9). In the folate *de novo* biosynthesis pathway, the pterin moiety formed from GTP is coupled to PABA by dihydropteroate synthase, the target of sulfonamides, leading to the formation of dihydropteroate, which is further modified by the addition of a glutamate moiety, generating dihydrofolate. Dihydrofolate is further catalyzed by dihydrofolate reductase, the target of trimethoprim (TMP), to form tetrahydrofolate, which is the parent structure of the large folate family of coenzymes.

In this study, we identified a two-gene operon necessary for *L. monocytogenes* PABA synthesis: *pabA* is predicted to encode the *para*-aminobenzoate synthase amidotransferase component, and *pabBC* is predicted to encode a bifunctional enzyme with both the *para*-aminobenzoate synthase aminase function and the aminodeoxychorismate lyase function. Although mutants in either *pabA* or *pabBC* grew normally in rich media, they required PABA for optimal growth in defined media lacking PABA and were severely attenuated for virulence in tissue culture models and in mice. We also report that PABA biosynthesis was upregulated by PrfA.

RESULTS

PABA is required for virulence of *L. monocytogenes* in mice. Two enzymes are predicted to catalyze PABA biosynthesis in *L. monocytogenes*: one is the glutamine amidotransferase (PabA in *Escherichia coli*) encoded by *Imo2749*, which functions during the first biosynthetic step together with an aminase. The other enzyme, encoded by *Imo2750*, is predicted to have both the *para*-aminobenzoate synthase aminase (PabB in *E. coli*) function and the aminodeoxychorismate lyase (PabC in *E. coli*) function and thereby participates in both steps to generate PABA. From here on, the gene *Imo2749* is named *pabA* and *Imo2750* is named *pabBC* based on their predicted functions (11–19).

To understand the importance of *L. monocytogenes* PABA biosynthesis, we used allelic exchange to introduce in-frame deletions into *pabA* or *pabBC*, and we evaluated their virulence by intravenous infection of mice. Compared to wild-type 10403S, the $\Delta pabA$ strain was approximately 50-fold defective and the $\Delta pabBC$ strain was about 180-fold less virulent as indicated by CFU in spleens, while in livers, virulence was attenuated 1,000-fold for the $\Delta pabA$ strain and 8,000-fold for the $\Delta pabBC$ strain (Fig. 1). The virulence defects were rescued by complementation with the corresponding genes (Fig. 1). These data indicated that *de novo* PABA biosynthesis is required for virulence of *L. monocytogenes* in mice.

PABA biosynthesis is required for extracellular and intracellular growth of *L. monocytogenes*. To achieve full virulence, *L. monocytogenes* needs to enter host cells, escape from the resultant phagosomes, grow intracellularly, nucleate the polymerization of host actin, and spread from cell to cell. Since PABA is the building block of folates (Fig. 2A), the virulence defects observed in the PABA-deficient strains were most likely due to growth defects caused by an inability to synthesize folates. To assess the importance of *de novo* PABA biosynthesis during bacterial growth, we first examined extracellular growth of the *pabA* and *pabBC* mutants. Although both mutants grew like the wild type in brain heart infusion (BHI) (see Fig. S1A in the supplemental material) and in complete listeria synthetic medium (cLSM) (Fig. S1B), $\Delta pabA$ and $\Delta pabBC$ strains were defective for growth in PABA-minus cLSM and the defects in the

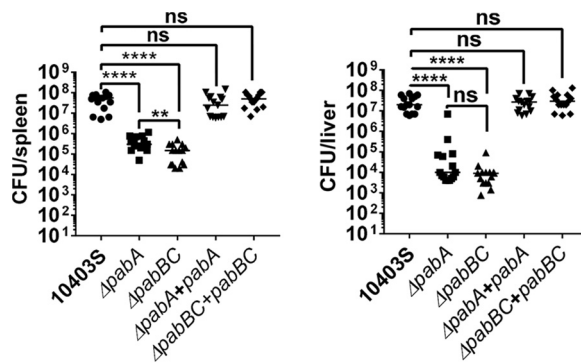


FIG 1 PABA is required for virulence of *L. monocytogenes* in mice. Wild-type female CD-1 mice were infected with 1×10^5 CFU of *L. monocytogenes* 10403S, $\Delta pabA$, $\Delta pabBC$, $\Delta pabA + pabA$, and $\Delta pabBC + pabBC$ strains, respectively, via intravenous (i.v.) injection. Homogenates of spleens or livers were plated and bacterial burden (CFU) per organ was enumerated at 48 h postinfection. Strains are as follows: $\Delta pabA + pabA$, $\Delta pabA$ strain complemented with *pabA* driven by its native promoter, and $\Delta pabBC + pabBC$, $\Delta pabBC$ strain complemented with *pabBC* driven by its native promoter. Data points and medians are results from two pooled experiments ($n = 15$). Each dot represents the CFU in one mouse. For all experiments, *P* values were calculated using an unpaired Student *t* test. **, $P < 0.01$; ****, $P < 0.0001$. ns, not significant.

$\Delta pabBC$ strain were much more severe (Fig. 2B). Since PabBC is predicted to be involved in both catalytic steps, it is reasonable that the *pabBC* deletion resulted in a complete loss of PABA biosynthesis and led to a more severe defect than the *pabA* deletion. Corresponding gene complementation (Fig. S1C) or supplementation with folic acid (FA), dihydrofolic acid (DHF), or tetrahydrofolic acid (THF) (Fig. 2C and D) restored growth of the deletion mutants. Moreover, trimethoprim (TMP) treatment inhibited growth of the wild-type and $\Delta pabA$ strains to an extent similar to that of the $\Delta pabBC$ strain (Fig. S1D). Treatment with sulfonamides (SMX) failed to inhibit growth, likely because the concentration of SMX did not compete with PABA supplementation in cLSM (Fig. S1D). Therefore, the lack of folate biosynthesis led to the growth defects of the PABA-deficient strains in PABA-minus cLSM.

The one-carbon units in CH₂-THF can be transferred to 10f-THF and subsequently used to synthesize purines, the first product of which is inosine mono-phosphate (IMP) (20). Rapidly proliferating cells synthesize larger amounts of DNA and RNA per unit time than do slowly dividing cells, leading us to wonder if growth defects of the deletions were due to an inability to synthesize purines. However, supplementation of IMP, saturated or not, did not fully restore growth of the $\Delta pabBC$ strain in PABA-minus medium (Fig. S1E and F), nor did supplementation with adenosine or guanosine, two downstream metabolites of IMP (Fig. S1G and H). In support of this *in vitro* observation, our previous report (21) showed that an *L. monocytogenes* adenine auxotroph was 1.5 logs less virulent than the wild-type parental strain *in vivo*, clearly not nearly as attenuated as the PABA-deficient mutants. Furthermore, addition of thymidine, another downstream metabolite of folate, did not promote growth of the PABA-deficient strains in broth (Fig. S1I). Therefore, other functions of folates were also required for growth of *L. monocytogenes* in synthetic medium.

Both the $\Delta pabA$ and $\Delta pabBC$ strains showed defects in intracellular growth in bone marrow-derived macrophages (BMMs) (Fig. 2E), and the defects were dramatically enhanced if the strains were first starved in PABA-minus cLSM (Fig. 2F and G). In addition, the intracellular growth defects of starved deletion strains were rescued by gene complementation (Fig. S1J), PABA supplementation (Fig. 2F), or DHF supplementation (Fig. 2G). The growth of wild-type bacteria in BMMs was inhibited by treatment with TMP (Fig. S1K), suggesting that PABA-dependent folate biosynthesis was required for intracellular growth.

PABA is required for optimal phagosomal escape and induction of actin polymerization by cytosolic *L. monocytogenes*. To replicate in the host cytosol, *L. monocytogenes* needs to first escape from phagosomes. It was noteworthy that the intracellular growth curves of the starved PABA-deficient strains resembled that of Δhly strains, which

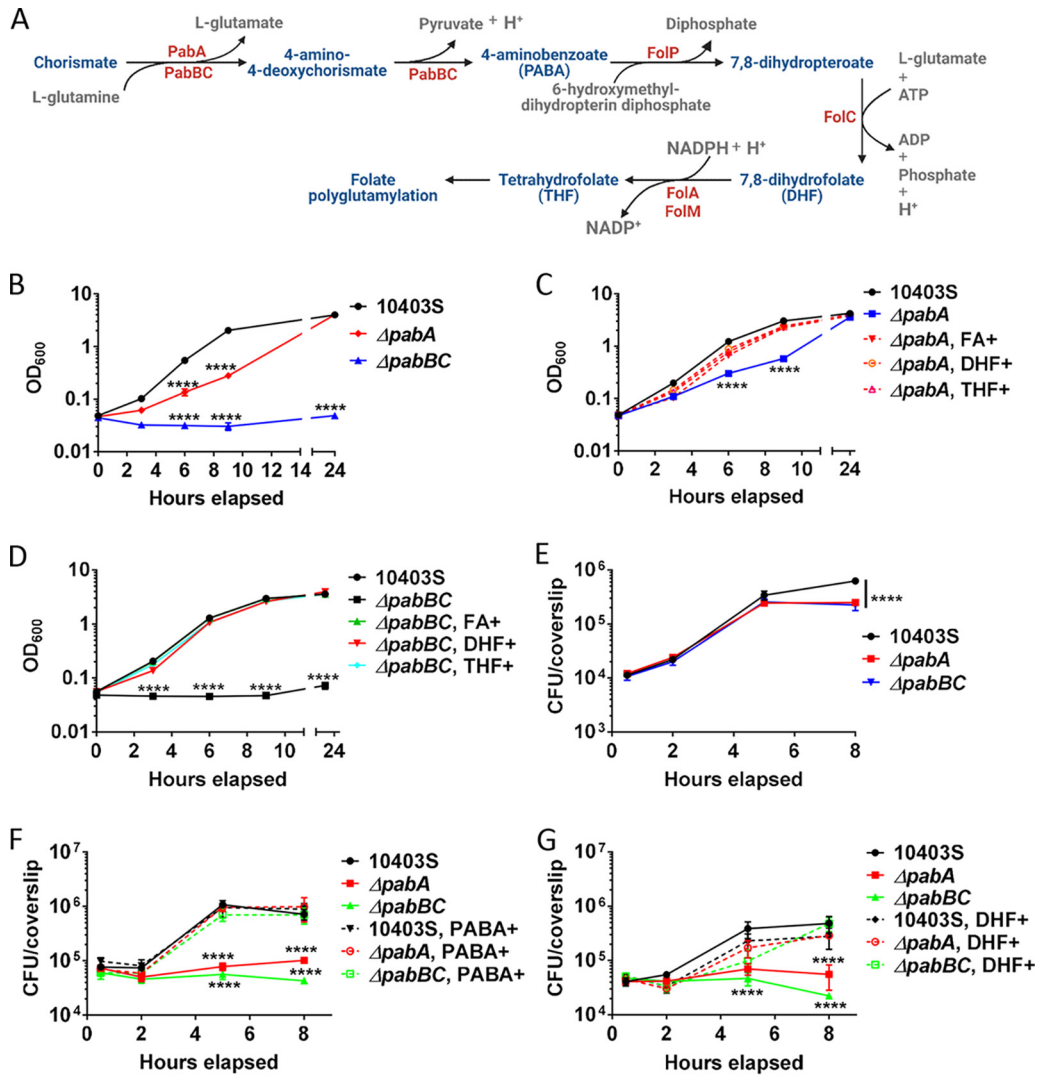


FIG 2 PABA biosynthesis is required for extracellular and intracellular growth of *L. monocytogenes*. (A) Tetrahydrofolate biosynthetic pathway in *L. monocytogenes*. Enzymes are colored red, main metabolic intermediates are colored blue, and others are colored gray. (B) *L. monocytogenes* 10403S, $\Delta pabA$, and $\Delta pabBC$ strains were starved in PABA-minus cLSM overnight at 37°C with shaking. The next day, starved strains were inoculated in cLSM without PABA and grown at 37°C with shaking. OD₆₀₀ was measured at different time points postinoculation as indicated over 24 h. (C and D) Prestarved wild-type 10403S, $\Delta pabA$, and $\Delta pabBC$ strains were grown in PABA-minus cLSM with or without 10 μg/mL of folic acid (FA), 10 μg/mL of dihydrofolic acid (DHF), or 10 μg/mL of tetrahydrofolic acid (THF) at 37°C with shaking. OD₆₀₀ was read at different time points postinoculation as indicated over 24 h. (E) *L. monocytogenes* 10403S, $\Delta pabA$, and $\Delta pabBC$ strains were grown overnight in BHI at 30°C. Intracellular growth was determined in wild-type C57BL/6J BMMs following infection at an MOI of 0.25. (F and G) Prestarved wild-type 10403S, $\Delta pabA$, and $\Delta pabBC$ strains were used for BMM infection at an MOI of 2.5. PABA (0.1 mg/mL) or DHF (10 μg/mL) was supplemented in cell culture medium at 30 min postinfection in indicated groups. Gentamicin (50 μg/mL) was added at 1 h postinfection. Growth curves are data pooled from three independent experiments. Error bars represent the standard deviations of the means of technical triplicates. For all experiments, *P* values were calculated using an unpaired Student *t* test. ****, *P* < 0.0001.

cannot escape from the phagosomes (Fig. 2F and G). To explore whether the intracellular growth defects we observed in starved PABA-deficient strains were also due to an inability to escape from phagosomes, we performed a phalloidin staining assay which is based on the observation that upon accessing the cytosol, wild-type *L. monocytogenes* induces the ActA-dependent polymerization of host actin that is labeled by fluorescent phalloidin (22–24). All *L. monocytogenes* strains expressed green fluorescent protein (GFP), host actin was labeled with phalloidin after 90 min of infection, and the percentage of phalloidin-positive, GFP-tagged bacteria was calculated. Not surprisingly, all of the strains colocalized with host actin normally (approximately 50%) after

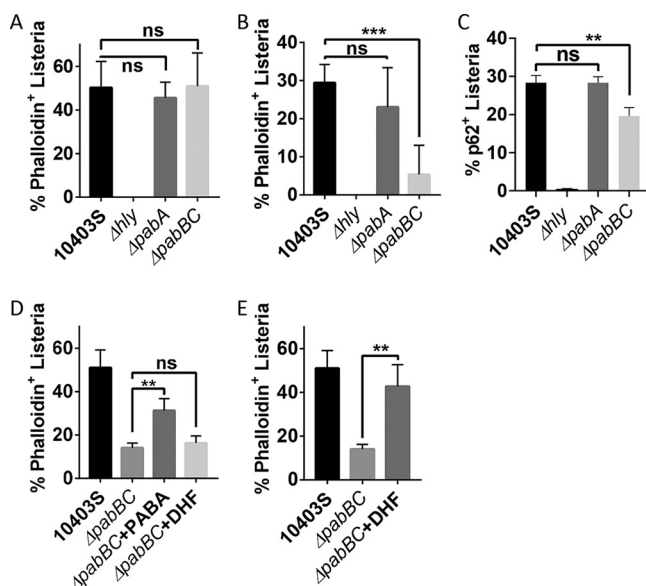


FIG 3 PABA is required for optimal phagosomal escape and induction of actin polymerization around cytosolic *L. monocytogenes*. (A to C) GFP-tagged wild-type 10403S, Δhly , $\Delta pabA$, and $\Delta pabBC$ strains were grown overnight in BHI at 30°C (A) or starved overnight in PABA-minus cLSM at 37°C with shaking (B and C). Wild-type C57BL/6J BMMs were infected with indicated strains at an MOI of 10. Gentamicin (50 μ g/mL) was added at 1 h postinfection. Cells were fixed and stained with phalloidin (A and B) or anti-p62 antibody (C) at 1.5 h postinfection. At least five images were taken and at least 100 bacteria were analyzed for each strain. The percentage of phalloidin-positive bacteria (A and B) or p62 colocalized bacteria (C) was calculated. Error bars represent the standard deviations of the means of technical triplicates pooled from three independent experiments. For all experiments, *P* values were calculated using an unpaired Student *t* test. **, *P* < 0.01; ***, *P* < 0.001. (D) Prestarved wild-type 10403S and the $\Delta pabBC$ strain were used for the phalloidin staining assay. All procedures were the same as for panel B except that PABA (0.1 mg/mL) or DHF (10 μ g/mL) was added as indicated at 30 min postinfection. (E) Wild-type 10403S and the $\Delta pabBC$ strain were grown overnight at 37°C with shaking in PABA-minus cLSM with or without supplementation of 10 μ g/mL of DHF. All the rest of the procedures were the same as for panel B.

growth overnight in BHI (Fig. 3A). However, after PABA starvation, while approximately 30% of wild-type bacteria stained with phalloidin, less than 5% of the PABA-starved $\Delta pabBC$ bacteria were phalloidin positive, suggesting either that they were unable to escape from the phagosomes or that they failed to have sufficient functional ActA to induce actin polymerization (Fig. 3B and Fig. S2). Therefore, we examined colocalization of *L. monocytogenes* with p62 as an alternative method to evaluate cytosolic localization (5, 25) and observed that approximately 20% of the $\Delta pabBC$ bacteria were p62 positive (Fig. 3C and Fig. S2), suggesting that these bacteria were in the cytosol but unable to induce host actin polymerization. Therefore, the growth defect of the starved $\Delta pabA$ strain in BMMs was attributed to its inability to propagate in the host cytosol, while that of the starved $\Delta pabBC$ was caused by its inability to escape from the phagosomes, move freely in the cytosol, and replicate intracellularly (Fig. 2D to G and Fig. 3B and C). Supplementation with PABA in cell culture medium 30 min postinfection rescued the actin colocalization defect of the starved $\Delta pabBC$ mutant, while supplementation of DHF in the cell culture medium did not (Fig. 3D), supporting previous reports that PABA is passively diffusive between membranes, while folates are actively transported (26–29). However, if PABA-minus, DHF-containing cLSM was used to grow the $\Delta pabBC$ strain prior to infection, the mutant was able to colocalize with actin effectively (Fig. 3E), suggesting that PABA-dependent folate synthesis promoted *L. monocytogenes* phagosomal escape and ActA-mediated movement. Additional work is needed to determine if the expression or function of ActA is regulated by PABA production.

PABA biosynthesis is activated by PrfA. PrfA regulates expression of *L. monocytogenes* virulence genes such as *hly* and *actA*, which mediate phagosomal escape and

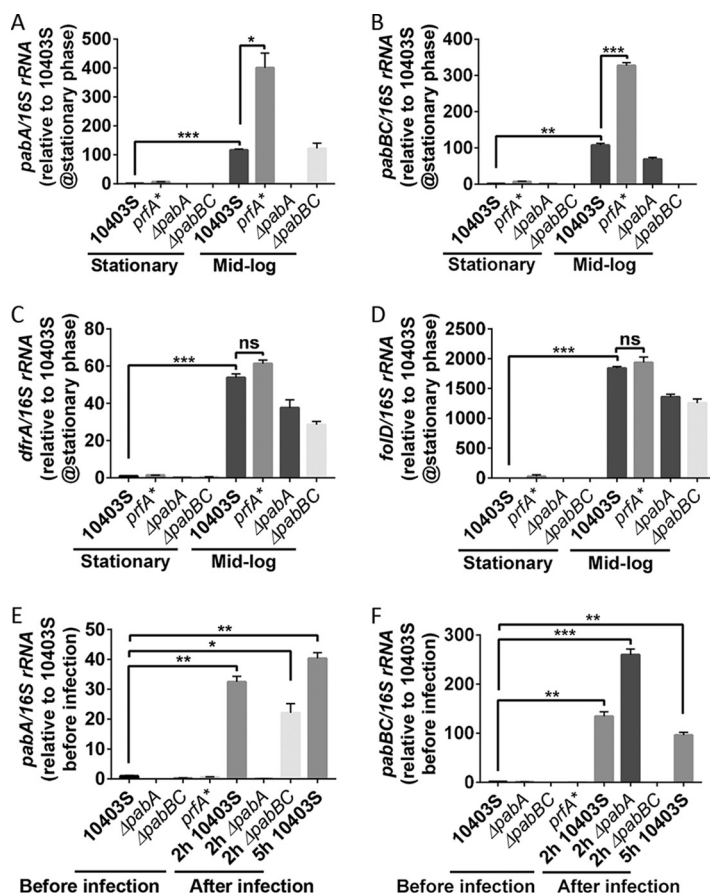


FIG 4 PABA biosynthesis is activated by PrfA. (A to D) Overnight-starved wild-type 10403S, *prfA**, Δ pabA, and Δ pabBC strains were back-diluted 1:10 in PABA-minus cLSM and grown for 2 h at 37°C with shaking to mid-log phase. For each strain, 0.5×10^9 CFU were collected right before and 2 h after subculturing as stationary-phase bacteria and log-phase bacteria, respectively. RNAs were extracted, reverse transcribed, and used for RT-qPCR analysis. Expression of the target gene was normalized to that of the 16S rRNA to compensate for any difference in the amount of samples. Fold change of the target gene in each sample relative to the stationary-phase 10403S sample was plotted. (E and F) Overnight-starved bacteria were used for BMM infection. Bacterial gene expression during BMM infection at an MOI of 40 was determined by RT-qPCR. Plotted data were normalized to the expression of 16S rRNA and were the fold change of the target gene in each sample relative to the wild-type 10403S before infection. Data are means and standard deviations of two technical replicates from two independent experiments. *P* values were calculated using an unpaired Student *t* test. *, *P* < 0.05; **, *P* < 0.01; ***, *P* < 0.001.

ActA-dependent actin polymerization, respectively. To determine if PrfA also regulates PABA production and/or folate metabolism, we analyzed expression of *pabA*, *pabBC*, *dfra* (*lmo1873*), and *folD* (*lmo1360*) in a *prfA** strain in which PrfA is locked in its active conformation due to a G145S point mutation. *dfra* encodes dihydrofolate reductase, which is involved in tetrahydrofolate synthesis, and *folD* encodes a bifunctional enzyme, FoLD (5,10-methylene-tetrahydrofolate dehydrogenase/5,10-methylene-tetrahydrofolate cyclohydrolase), that is involved in tetrahydrofolate interconversion and one-carbon metabolism. Although expression of all genes was upregulated during rapid mid-log growth in wild-type 10403S, PrfA upregulated expression of both *pabA* and *pabBC* but not *dfra* or *folD* in mid-log-phase *prfA** cultures compared to mid-log wild type (Fig. 4A to D), suggesting that PABA production was upregulated by PrfA. Interestingly, constitutive expression of PrfA increased *pabA* and *pabBC* expression in PABA-minus cLSM but not in BHI, suggesting that the absence of PABA or other nutrients is a prerequisite for the regulation of PrfA for PABA biosynthesis (Fig. S3). Consistent with PrfA being upregulated during infection, expression of *pabA* and *pabBC* was increased upon infection in BMMs (Fig. 4E and F). Taken together, these data suggest that PrfA increased PABA production during infection.

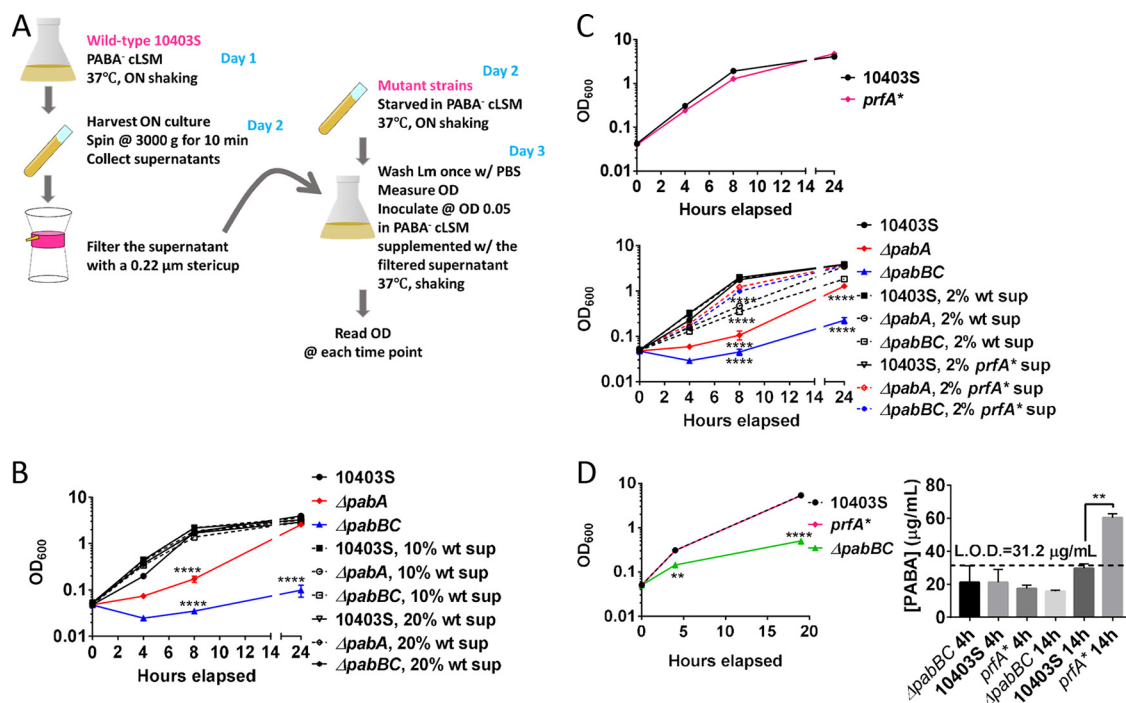


FIG 5 PABA is released from *L. monocytogenes* and the process is enhanced by PrfA activation. (A) Schematic diagram of how the supernatant rescue assay was conducted. (B) Rescue of growth of PABA-deficient strains in PABA-minus cLSM by supplementation of supernatants collected from wild-type 10403S cultures. The final concentration of wild-type supernatant in PABA-minus cLSM was either 10% or 20% as indicated. (C) Growth of wild-type 10403S and *prfA** strains in PABA-minus cLSM at 37°C with shaking was monitored and supernatants were collected and used at 2% for the rescue assay. (D) Prestarved overnight cultures of wild-type 10403S, *prfA**, and $\Delta pabBC$ strains were inoculated in PABA-minus cLSM at an initial OD₆₀₀ of 0.05 and cultured at 37°C with shaking. OD₆₀₀ was measured and supernatants were collected at indicated time points. PABA concentration was measured using a commercial ELISA kit. L.O.D., limit of detection. Growth curves and ELISA results were generated from two independent experiments. Error bars represent the standard deviations of the means of technical triplicates. For all experiments, *P* values were calculated using an unpaired Student *t* test. **, *P* < 0.01; ****, *P* < 0.0001.

PABA can passively diffuse between cell membranes (26–28). Accordingly, we designed a PABA rescue assay using supernatant fluids from overnight cultures of wild-type or *prfA** strains grown in PABA-minus cLSM, which were then filtered and supplemented in PABA-minus cLSM at different ratios. These conditional media were used for *in vitro* growth analysis of the PABA-deficient strains (Fig. 5A). Supplementation with 10% wild-type supernatant fluid was sufficient to restore the growth of PABA-deficient strains (Fig. 5B). Furthermore, growth with 2% *prfA** supernatant fluid was better than growth with 2% wild-type supernatant fluid, supporting the idea that PABA was released from the bacteria and that PrfA up-regulated PABA synthesis (Fig. 5C).

We next measured PABA concentrations in supernatants of bacterial cultures and were able to detect PABA only in supernatants from *prfA** strains collected during stationary phase (Fig. 5D), suggesting that PABA was present outside the bacteria and that PrfA increased PABA production.

Increase of (p)ppGpp promotes phagosomal escape and actin polymerization of PABA-deficient *L. monocytogenes*. The plaque assay is one of the best assays to recapitulate pathogenesis of *L. monocytogenes in vitro*; in this assay, a monolayer of fibroblasts is infected with *L. monocytogenes* and plaques form 2 to 3 days postinfection due to cell death caused by bacterial growth and spread from cell to cell. Bacteria that are defective in phagosomal escape, intracellular growth, and/or cell-to-cell spread form smaller plaques than the wild type. Consistent with the *in vivo* virulence assay, the phalloidin staining assay, the p62 staining assay, and the BMM growth curve results, $\Delta pabA$ *L. monocytogenes* formed tiny plaques and the $\Delta pabBC$ strain showed no plaques at all, both of which were rescued by gene complementation (Fig. 6A) or PABA supplementation (Fig. 6B).

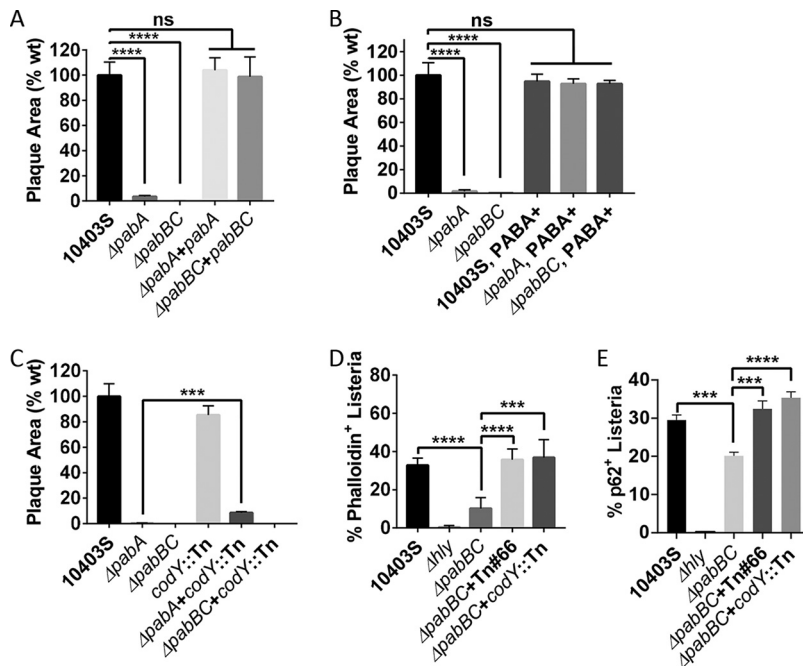


FIG 6 Increase of (p)ppGpp promotes phagosomal escape and actin polymerization of PABA-deficient *L. monocytogenes*. (A to C) Plaque area measured 3 days postinfection as a percentage of wild-type 10403S. In panel B, PABA was added at 0.1 mg/mL at 1 h postinfection as indicated. $\Delta pabA + codY::Tn$, $\Delta pabA$ strain carrying a *codY* transposon mutation; $\Delta pabBC + codY::Tn$, $\Delta pabBC$ strain carrying a *codY* transposon mutation. Error bars represent the standard deviations of the means ($n = 10$) from two independent experiments. (D and E) Phalloidin staining assay (D) and p62 staining assay (E) using prestarved GFP-tagged *L. monocytogenes* strains. $\Delta pabBC + Tn66$, $\Delta pabBC$ strain carrying a transposon mutation targeting at *relA*. At least five images were taken and at least 100 bacteria were analyzed for each strain. Error bars represent the standard deviations of the means of technical triplicates pooled from two independent experiments. For all experiments, P values were calculated using an unpaired Student t test. ***, $P < 0.001$; ****, $P < 0.0001$.

To explore the regulatory mechanisms in PABA-mediated pathogenesis, we screened for transposon mutants in a $\Delta pabA$ background that formed larger plaques. Seven transposon mutants were identified that formed significantly larger plaques than those of the parental strain, but none of these strains formed plaques that were comparable to those of the wild type (Fig. S4A). The transposon target sites and the sizes of the plaques compared to those of the wild type are listed in Fig. S4B. Among the transposon insertion mutants, the two in *relA* attracted our attention. RelA is a bifunctional enzyme that contains both a (p)ppGpp synthase domain and a hydrolase domain that orchestrate the levels of (p)ppGpp in response to starvation and other stressors (30). The net outcome of a *relA* deletion in *L. monocytogenes* is the increase of (p)ppGpp because there are two other enzymes that can synthesize (p)ppGpp, while RelA is the only protein that has (p)ppGpp hydrolase activity (31–34). Since two transposons inserted at two different sites in *relA*, one located near the ribosome binding site and the other targeted at the C-terminal regulatory domain (Fig. S4B), we hypothesized that the rescue of plaque formation by insertions Tn66 and Tn48 was attributed to the disruption/loss of function of the whole gene leading to an increase of (p)ppGpp. One of the major targets of (p)ppGpp is CodY (35). CodY is a suppressor of many biosynthetic genes, and (p)ppGpp blocks the repressor function of CodY. Indeed, similar to the case with *relA* mutation, disruption of *codY* by a transposon mutation in *codY* partially restored the plaque forming ability of the $\Delta pabA$ strain (Fig. 6C), suggesting that RelA and thereby CodY negatively regulated pathogenesis in the absence of PABA.

To determine at which stage RelA or CodY disruption promoted pathogenesis of PABA-deficient strains, we performed phalloidin and p62 staining assays and found that deletion of *relA* or *codY* restored phagosomal escape and induction of actin

polymerization of the $\Delta pabBC$ strain (Fig. 6D and E). However, analysis of bacterial growth in PABA-minus cLSM showed that deficiency of *relA* or *codY* had little benefit for the growth of the $\Delta pabA$ or $\Delta pabBC$ strain (Fig. S4C). Consistently, absence of *relA* or *codY* was unable to rescue the virulence defects of PABA-deficient strains in mice (Fig. S4D). Therefore, deletion of *relA* or *codY* promoted pathogenesis of PABA-insufficient strains by an increase of phagosomal escape and actin polymerization. However, the strain lacking both *pabBC* and *codY* was still unable to grow *in vitro* or *in vivo*.

DISCUSSION

The results of this study identified two *L. monocytogenes* genes (*pabA* and *pabBC*) required for PABA biosynthesis. *L. monocytogenes* mutants lacking these genes were unable to grow in synthetic medium lacking PABA but had no measurable growth defect in rich medium (BHI). The mutants were highly attenuated for virulence in mice (Fig. 1) and had profound defects during intracellular growth in tissue culture models of infection. These results were not surprising since PABA is an essential component of folic acid biosynthesis and the target of sulfonamide antibiotics drugs used to treat many bacterial infections, including listeriosis (9). Further analysis revealed that the virulence defects were caused by the inability of the mutants to produce folic acid and its downstream metabolites, such as tetrahydrofolates, that are essential for 1-carbon metabolism. During infection, mutants in PABA biosynthesis had defects in phagosomal escape, replication, and induction of host actin polymerization (Fig. 2 and 3). Our study also showed that *pabA* and *pabBC* expression was induced during infection and partially under the control of the master transcriptional regulator of *L. monocytogenes* virulence (PrfA) (Fig. 4 and 5).

Most bacteria can synthesize PABA, although the details vary. In *E. coli*, PABA production occurs in two steps catalyzed by three enzymes (PabA to -C). PabA and PabB participate in the first step to generate 4-amino-4-deoxychorismate, although PabA functions only in the presence of PabB, while PabB can function at a reduced rate in the absence of PabA by utilizing ammonia (12, 15, 18). In sharp contrast to PabA and PabB, both of which show sequence and functional similarities to the large and small subunits of anthranilate synthase, respectively (36, 37), PabC converts 4-amino-4-deoxychorismate to PABA and has no counterparts in anthranilate biosynthesis and is thus unique to the PABA biosynthetic pathway (12–14). This “three-gene” system is also used by *Bacillus subtilis*, in which *trpG*, *pab*, and *pabC* are homologs of *E. coli* *pabA*, *pabB*, and *pabC* (19). However, only two genes (*pabA* and *pabBC*) are predicted to be required for PABA biosynthesis in *L. monocytogenes* 10403S; the former encodes glutamine amidotransferase, similar to *E. coli* *pabA*, and the latter encodes a fused enzyme harboring both an aminase domain which catalyzes the first step of the reaction (similar to PabB) and a lyase domain for the second step of the reaction (similar to PabC). Based on these predictions, an *L. monocytogenes* $\Delta pabA$ mutant is only partially PABA deficient because its deficiency is likely compensated by its counterpart in anthranilate synthase, and PabBC is able to function without PabA, although at a reduced rate. However, a $\Delta pabBC$ mutant is a complete PABA-null mutant because it lacks the unique enzymatic function of PabC. Indeed, the $\Delta pabBC$ mutant had more severe defects in extracellular and intracellular growth, phagosomal escape, actin polymerization, and virulence than did the $\Delta pabA$ mutant (Fig. 2, 3, and 6).

There is no question that *L. monocytogenes* requires PABA biosynthesis for pathogenesis, but the $\Delta pabA$ and $\Delta pabBC$ mutants grew normally in BHI, which is totally derived from animal products and therefore should lack PABA. However, since folates are vulnerable to degradation (38, 39), we suspect that folates present in BHI are degraded to PABA and provide a sufficient amount of PABA to promote growth. Although the $\Delta pabA$ and $\Delta pabBC$ mutants required PABA in synthetic medium, growth was restored by the addition of dihydrofolate (DHF) or tetrahydrofolate (THF), thereby raising the question of why these mutants cannot grow intracellularly. One likely explanation is that folates imported into mammalian cells are modified by polyglutamation, a strategy used by

mammalian cells to prevent loss of these nutrients (40). Some bacteria, for example, *Lactobacillus casei*, import pteroylmonoglutamates more efficiently than pteroylpolyglutamates (29). Therefore, it was likely that *L. monocytogenes* could not use host folates because they were highly polyglutamated but could use supplemented folates because they were not polyglutamated.

PrfA is the major regulator in *L. monocytogenes* that directly stimulates the expression of virulence factors, including LLO, PlcA, PlcB, Mpl, ActA, InlA, InlB, InlC, Bsh, and UhpT (41–48). PrfA is not required for growth of *L. monocytogenes* in BHI but is highly upregulated during infection (41, 49, 50). To study activated PrfA in medium, we often use a strain with a mutation that locks PrfA in its active conformation (*prfA**) (6, 51, 52). Although the *pabA* and *pabBC* operon lacks a PrfA binding site in its promoter, we found that *prfA** strains upregulated PABA production in PABA-minus synthetic media (Fig. 4A and B and Fig. 5C and D) but not in rich BHI medium (Fig. S3). Furthermore, both *pabA* and *pabBC* were upregulated during infection (Fig. 4E and F). To gain further insight into the regulation of PABA biosynthesis, we performed a suppressor screen looking for transposon mutants that rescued the small-plaque phenotype of $\Delta pabA$ mutants. We identified two independent *relA* mutants that, as discussed in Results, are predicted to have higher levels of (p)ppGpp (31–35) and are therefore predicted to inactivate CodY, which is a repressor of many biosynthetic genes (35). Both *relA* and *codY* mutations restored the plaque forming ability of the $\Delta pabA$ bacteria significantly, although they did not restore virulence in mice (Fig. 6C and Fig. S4A and D). CodY also regulates *prfA* transcription by directly binding to the coding sequence 15 nucleotides downstream of the start codon (53). Although CodY upregulates *prfA* transcription specifically under low concentrations of branched-chain amino acids (BCAAs) (53, 54), in the scenario of PABA deficiency, RelA and downstream CodY negatively regulated phagosomal escape and actin polymerization within the first 2 h postinfection (Fig. 6D and E), though the detailed regulatory mechanisms among PABA, CodY, and PrfA are unknown. The differential regulation of CodY under different conditions should be spatiotemporally dependent and still awaits further exploration.

The results of this study clearly show that PABA biosynthesis is essential for *L. monocytogenes* pathogenesis and is upregulated during infection and that *prfA** strains secrete PABA into the growth medium. We wondered if secreted PABA might have other biological roles and found a few intriguing reports in the literature to consider. For example, PABA may act as a pathogen-associated molecular pattern (PAMP) in that it is essential, conserved, and secreted by bacteria but not made by the host (55–57). In one study, PABA induced interferon production in human peripheral blood cells and in mice (58, 59). Curiously, chemically synthesized PABA inhibits coenzyme Q biosynthesis in mammalian cells by binding competitively to CoQ2 (60, 61). Thus, it is possible that PABA secreted by *L. monocytogenes* and other pathogens may affect host cell metabolism and/or act as a PAMP that stimulates the host immune system.

MATERIALS AND METHODS

Bacterial strains and growth conditions *in vitro*. All strains used in this study are listed in Tables 1 and 2. *L. monocytogenes* 10403S (DP-L6253) is referred to as the wild-type strain, and all other strains are isogenic derivatives of this parental strain. Unless otherwise stated, all *L. monocytogenes* strains were cultivated overnight in brain heart infusion (BHI) medium at 30°C or grown on BHI plates at 37°C with streptomycin and all *E. coli* strains were grown in Luria broth (LB) at 37°C with shaking or on LB plates at 37°C. Antibiotics were used at the following concentrations: streptomycin, 200 $\mu\text{g}/\text{mL}$; erythromycin, 1 $\mu\text{g}/\text{mL}$; carbenicillin, 100 $\mu\text{g}/\text{mL}$; and chloramphenicol, 7.5 $\mu\text{g}/\text{mL}$ for *L. monocytogenes* and 10 $\mu\text{g}/\text{mL}$ for *E. coli*.

Cloning and strain construction. Plasmids were introduced by conjugation into *L. monocytogenes* by mating with *E. coli* strain SM10 (62). Gene complementation was achieved as previously described (63) by cloning genes into the phage integration vector pPL2 using the native promoter (for *pabA* or *pabBC* complementation) or a Hypher promoter (for GFP expression). In-frame deletions of genes in *L. monocytogenes* were performed by allelic exchange (64) using the plasmid pKSV7. Briefly, the left arm and right arm flanking the deletion portion were cloned into pKSV7 and the constructed plasmid was transformed into *E. coli* XL1 Blue and later SM10 and then conjugated into *L. monocytogenes*. *L. monocytogenes* organisms carrying the plasmid were then selected on streptomycin and chloramphenicol BHI plates at 30°C and restreaked at 42°C three consecutive times on streptomycin and chloramphenicol BHI

TABLE 1 *L. monocytogenes* strains

Strain	Description	Reference
DP-L6253	Wild-type 10403S	68
DP-L5451	<i>prfA</i> *	69
DP-L7454	$\Delta pabA$	This study
DP-L7455	$\Delta pabA + pabA$	This study
DP-L7456	$\Delta pabBC$	This study
DP-L7457	$\Delta pabBC + pabBC$	This study
DP-L7458	10403S-GFP	This study
DP-L7459	Δhly -GFP	This study
DP-L7460	$\Delta pabA$ -GFP	This study
DP-L7461	$\Delta pabBC$ -GFP	This study
DP-L7462	10403S + Tn1	This study
DP-L7463	10403S + Tn5	This study
DP-L7464	10403S + Tn13	This study
DP-L7465	10403S + Tn24	This study
DP-L7466	10403S + Tn48	This study
DP-L7467	10403S + Tn57	This study
DP-L7468	10403S + Tn66	This study
DP-L7469	$\Delta pabA + Tn1$	This study
DP-L7470	$\Delta pabA + Tn5$	This study
DP-L7471	$\Delta pabA + Tn13$	This study
DP-L7472	$\Delta pabA + Tn24$	This study
DP-L7473	$\Delta pabA + Tn48$	This study
DP-L7474	$\Delta pabA + Tn57$	This study
DP-L7475	$\Delta pabA + Tn66$	This study
DP-L7476	$\Delta pabBC + Tn66$	This study
DP-L7477	10403S + <i>codY</i> ::Tn	This study
DP-L7478	$\Delta pabA + codY::Tn$	This study
DP-L7479	$\Delta pabBC + codY::Tn$	This study
DP-L7480	$\Delta pabBC + Tn66$ -GFP	This study
DP-L7481	$\Delta pabBC + codY::Tn-GFP$	This study

plates to select for chromosomal integration. Single colonies were then picked and serially passaged at 30°C with shaking to facilitate loss of pKSV7. Deletion strains that lost the plasmid were identified by patch-plating methods and confirmed by PCR and Sanger sequencing.

Virulence assay in mice. The virulence assay was carried out in strict accordance with the recommendations in the *Guide for the Care and Use of Laboratory Animals* (65). All procedures were reviewed and approved by the Institutional Animal Care and Use Committee (IACUC) at the University of California, Berkeley, under protocol AUP-2016-05-8811. *L. monocytogenes* strains were cultured overnight in 2.5 mL of streptomycin-containing BHI liquid medium and grown at 30°C lying horizontally in 15-mL conical tubes. The overnight cultures were diluted 1:10 into fresh streptomycin-containing BHI medium the next day and grown to mid-log phase at 37°C with shaking (grown for about 2 h to an optical density at 600 nm [OD₆₀₀] of 0.5 to 1.5). Eight-week-old female CD1 mice (Charles River Laboratories) were then infected intravenously via the tail vein with 1×10^5 CFU of the mid-log-phase cultures in 200 μ L of sterile phosphate-buffered saline (PBS). All strains were plated on streptomycin-containing LB plates for the calculation and verification of the inoculum. After 48 h postinfection, mice were euthanized, and spleens and livers were harvested in 0.1% Nonidet P-40 in water, homogenized, and plated on LB agar plates with streptomycin to enumerate CFU and quantify bacterial burden per organ.

Growth curves in broth. For growth curves in BHI, strains were grown overnight at 30°C. The next day, bacteria were washed with PBS and diluted in fresh BHI to an OD₆₀₀ of 0.05. Strains were then cultured at 37°C with shaking, and OD was measured at indicated time points. For growth curves in

TABLE 2 *E. coli* strains

Strain	Plasmid or genotype	Reference
XL1-Blue	For cloning; <i>recA1 endA1 gyrA96 thi-1 hsdR17 supE44 relA1 lac</i> [F' <i>proAB lacI^q Z</i> Δ M15 Tn10 (Tet ^r)]	Stratagene
SM10	For conjugation; <i>thi-1 thr-1 leuB6 tonA21 lacY1 supE44 recA</i> λ^- integrated [RP4-2-Tcr::Mu] <i>aphA⁺</i> (Km ^r) Tra ⁺	62
DP-E6333	pPL2t	35
DP-E5228	pPL2-GFP	Lab strain
DP-E6324	pKSV7- <i>oriT</i>	64
DP-E7482	pPL2- <i>pabA</i>	This study
DP-E7483	pPL2- <i>pabBC</i>	This study
DP-E7484	pKSV7- $\Delta pabA$	This study
DP-E7485	pKSV7- $\Delta pabBC$	This study

complete listeria synthetic medium (cLSM) with or without 1 $\mu\text{g}/\text{mL}$ of PABA, strains were grown in PABA-minus cLSM overnight at 37°C with shaking. The next day, bacteria were washed once with PBS and diluted in fresh cLSM with or without PABA (1 $\mu\text{g}/\text{mL}$), folic acid (FA; 10 $\mu\text{g}/\text{mL}$), dihydrofolic acid (DHF; 10 $\mu\text{g}/\text{mL}$), tetrahydrofolic acid (THF; 10 $\mu\text{g}/\text{mL}$), IMP disodium (400 μM), trimethoprim (TMP; 2 $\mu\text{g}/\text{mL}$), or sulfamethoxazole (SMX; 60 $\mu\text{g}/\text{mL}$) to an OD_{600} of 0.05. Strains were then cultured at 37°C with shaking, and OD was read at time points as indicated.

Intracellular growth curves. Bone marrow-derived macrophages (BMMs) were prepared from 8- to 12-week-old female C57BL/6 mice (Jackson Laboratory) and cultivated in Dulbecco's Modified Eagle Medium (DMEM) containing 20% fetal bovine serum (FBS), 2 mM L-glutamine, 1 mM sodium pyruvate, 0.1% 2-mercaptoethanol, and 10% colony-stimulating factor (CSF) from macrophage colony-stimulating factor (M-CSF)-producing 3T3 cells. For each curve, a total of 3×10^6 BMMs were seeded and cultured overnight in a 60-mm petri dish containing 14 12-mm sterile glass coverslips. Bacterial overnight cultures were prepared on the same day in BHI medium at 30°C or prestarved in PABA-minus cLSM at 37°C with shaking as indicated. The next day, overnight cultures were washed with PBS once and used to infect BMMs for 30 min at a multiplicity of infection (MOI) of 0.25 for BHI cultures or an MOI of 2.5 for starved cultures. At 30 min postinfection, BMMs were washed twice with PBS and fresh medium was added. For indicated experiments, 0.1 mg/mL of PABA, 10 $\mu\text{g}/\text{mL}$ of DHF, 2 $\mu\text{g}/\text{mL}$ of TMP, or 60 $\mu\text{g}/\text{mL}$ of SMX was supplemented in cell culture medium at this time. At 1 h postinfection, 50 $\mu\text{g}/\text{mL}$ of gentamicin was added to the cell cultures. Three coverslips were removed at each time point and rigorously vortexed in sterile water for 30 s. An appropriate amount of the lysates was then plated on LB plates. Each set of data represents the average of three coverslips per time point per treatment per *L. monocytogenes* strain.

Phalloidin staining assay and p62 staining assay. On day 1, 2×10^5 wild-type C57BL/6 BMMs were seeded on a sterile 12-mm coverslip in 1 well of a 24-well plate containing 500 μL of BMM medium and overnight cultures of different GFP-tagged *L. monocytogenes* strains grown in BHI medium at 30°C or in PABA-minus cLSM at 37°C with shaking. Bacteria were grown overnight in PABA-minus DHF-plus (10 $\mu\text{g}/\text{mL}$) cLSM at 37°C with shaking when indicated. The next day, for p62 staining, BMMs were pretreated with 250 ng/mL of cytochalasin D (Sigma) 30 min prior to infection to prevent actin polymerization and allow for p62 staining (25). BMMs were infected with the overnight cultures at an MOI of 10. At 30 min postinfection, cells were washed twice with PBS and fresh medium was added with or without 0.1 mg/mL of PABA or 10 $\mu\text{g}/\text{mL}$ of DHF. For p62 staining, fresh medium with cytochalasin D was used. Gentamicin (50 $\mu\text{g}/\text{mL}$) was added at 1 h postinfection. After infection for 1.5 h, cells were washed twice with PBS and fixed in 4% paraformaldehyde (PFA) in PBS for 15 min at room temperature. After two washes with PBS, cells were permeabilized in BP buffer (0.1% saponin and 2% bovine serum albumin [BSA] in PBS) for 30 min at room temperature. From here on, steps were different for different types of staining. For the phalloidin staining, after two washes in PBS containing 0.1% saponin, phalloidin (Alexa Fluor 647 far red; Invitrogen; A22287) was diluted 1:500 in BP buffer and cells were stained at room temperature for 1 h. Coverslips were protected from light from then on. For the p62 staining, primary antibody (1:200 of guinea pig anti-p62 antibody; Fitzgerald; 20R-PP001) in BP buffer was added and incubated at room temperature for 90 min. Cells were washed with PBS containing 0.1% saponin six times, and then secondary antibody (1:2,000 of Alexa Fluor 647 goat anti-guinea pig IgG; Invitrogen; A21450) in BP buffer was added and incubated at room temperature for 1 h. Coverslips were protected from light from then on. After staining, all coverslips were washed with PBS containing 0.1% saponin three times and then PBS three times. Coverslips were then dried, mounted on a slide in a drop of ProLong gold plus 4',6-diamidino-2-phenylindole (DAPI) to stain the nuclei, and cured for 24 h at room temperature in the dark. At least five images were taken for each coverslip using Keyence equipped with four filters: a DAPI channel for the BMM nuclei, a GFP channel for *L. monocytogenes*, a Cy5 channel for phalloidin-labeled actin or p62 staining, and a bright-field channel to reveal the overall morphology of the cells.

RNA extraction and RT-qPCR. For transcriptional analysis of mid-log-phase bacteria in defined media, overnight cultures were prepared in PABA-minus cLSM at 37°C with shaking. Overnight cultures were back-diluted 1:10 the next day in fresh PABA-minus cLSM and grown for 2 h at 37°C with shaking to mid-logarithmic phase. While waiting, 0.5×10^9 CFU of each overnight culture were collected as stationary-phase controls before subculture, pelleted, and frozen at -20°C for RNA extraction together with the following samples. Mid-log-phase cultures were harvested and washed once with PBS, and a total of 0.5×10^9 CFU of each strain were used for RNA extraction following the manufacturer's instructions (Quick RNA fungal/bacterial miniprep kit; Zymo Research; R2014). DNase treatment was applied using TURBO DNase (Invitrogen) at 37°C for 30 min. An RNA clean and concentrate kit (Zymo Research; R2017) was used as instructed by the manufacturer, followed by the reverse transcription (RT) using iScript reverse transcription supermix (Bio-Rad). cDNAs were diluted and used for RT-quantitative PCR (qPCR) analysis using KAPA SYBR Fast qPCR kit Master Mix ($2 \times$) Universal. The 16S rRNA was used as the reference gene, and the target and reference genes had similar amplification efficiencies. Expression of the target gene was normalized to that of 16S rRNA to compensate for any difference in the concentration of samples in every run of qPCR. The threshold cycle ($2^{-\Delta\Delta\text{CT}}$) method was used and the fold change of the target gene in each sample relative to the stationary-phase wild-type sample was plotted. Sample preparation for transcriptional analysis during infection was performed as previously described (6). Briefly, 3×10^7 BMMs were seeded in each 150-mm tissue culture (TC)-treated dish and infected at an MOI of 40 with *L. monocytogenes* strains prestarved overnight in PABA-minus cLSM at 37°C with shaking. Meanwhile, 0.5×10^9 CFU of each overnight culture were collected as stationary-phase controls before infection, pelleted, and frozen at -20°C for RNA extraction together with the following samples. One hour postinfection, cells were washed twice with PBS, and prewarmed fresh BMM medium containing

50 $\mu\text{g}/\text{mL}$ of gentamicin was added. About 2 h postinfection, BMMs were gently washed once with PBS and 5 mL of chilled 0.1% NP-40 in water was added. Cells were lysed at 4°C for 5 to 10 min. All steps from this point on should be performed on ice. Lysates were collected in 15-mL tubes and vortexed for 10 s. Five milliliters of chilled RNAProtect bacterial reagent was used to rinse the dishes and was added to each tube, and the solution was completely mixed, followed by centrifugation at 4,000 rpm for 10 min at 4°C. The pellets were resuspended in 500 μL of 0.1% NP-40 in water and vortexed. One milliliter of RNAProtect bacterial reagent was added, and the tubes were spun at maximum speed at 4°C for 3 min. Supernatants were discarded and pellets were subjected to RNA extraction and analysis processes as described above.

Plaque assay and suppressor screen. For a routine plaque assay, details were described previously (66). Briefly, 1.2×10^6 L2 rat fibroblasts were seeded in 1 well of a 6-well plate and were infected at an MOI of 0.2 with overnight cultures prepared in BHI medium at 30°C. One hour postinfection, cells were washed twice with PBS, and 3 mL of “day 2 mix” with or without 0.1 mg/mL of PABA was added (1.5 mL of 2 \times DMEM, 1.5 mL of 1.4% agarose in water, and 10 $\mu\text{g}/\text{mL}$ of gentamicin). Forty-eight hours postinfection, 2 mL of staining mix with or without 0.1 mg/mL of PABA was added (1 mL of 2 \times DMEM, 1 mL of 1.4% agarose in water, 50 μL of neutral red solution, and 10 $\mu\text{g}/\text{mL}$ of gentamicin). Plaques were imaged 72 h postinfection, and plaque area was analyzed using ImageJ software. For a suppressor screen, a *himar-1* transposon library (67) composed of approximately 1×10^8 transposon mutants in a ΔpabA background was used to screen for transposon insertions that produced a larger plaque than the parental ΔpabA strain. For the initial screen, 7.2×10^6 L2 cells were seeded in one 10-cm TC dish and infected at an MOI of 0.1. A total of 30 dishes were screened. The plaque assay was then performed as described above except that the amount of all reagents was adjusted to match the 10-cm dishes. Selected large-plaque mutants were purified by scratching the selected plaques from the 10-cm dishes, culturing the strains in BHI medium, and repeating the plaque assay until the large-plaque phenotype was completely homogenous. Selected transposon mutants were sequenced and transduced into a wild-type 104035 background and a ΔpabA background, respectively, to confirm the large-plaque phenotype for the third time.

PABA concentration measurement. Overnight cultures of the indicated strains were prepared in PABA-minus cLSM at 37°C with shaking. The cultures were then back-diluted in PABA-minus cLSM to an initial OD of 0.05 and grown at 37°C with shaking for 4 h to mid-log phase or for 14 h to stationary phase. At the desired time points, OD was measured and used for the growth curve analysis, and bacterial cultures were harvested and spun down at 3,000 rpm for 10 min. Supernatants were collected, filtered with 0.22- μm Stericup filters, and stored at -20°C until measurement. Enzyme-linked immunosorbent assay (ELISA) was conducted following the manufacturer’s instructions (MyBioSource; MBS9303796).

Supernatant rescue assay. On day 1, wild-type and/or *prfA** *L. monocytogenes* strains were grown overnight in cLSM lacking PABA at 37°C with shaking. The next day (day 2), supernatants of the overnight cultures were harvested by centrifugation at $3,000 \times g$ for 10 min, filtered through a 0.22- μm -pore-size Stericup filter, and then used to supplement PABA-minus cLSM at different concentrations (volume per volume) as indicated. Also on day 2, mutant strains as well as their wild-type control strain were starved overnight in PABA-minus cLSM at 37°C with shaking. On day 3, the “day 2 overnights” were washed once with PBS and inoculated in supernatant-supplemented PABA-minus cLSM to an initial optical density at 600 nm (OD_{600}) of 0.05. Inocula were then cultured at 37°C with shaking, and OD_{600} was measured using a spectrophotometer at different time points as indicated.

Statistical analysis. Data were analyzed using GraphPad Prism 8.

SUPPLEMENTAL MATERIAL

Supplemental material is available online only.

SUPPLEMENTAL FILE 1, PDF file, 0.7 MB.

ACKNOWLEDGMENTS

This work was supported by National Institutes of Health grants 1P01AI063302 (D.A.P.) and 1R01AI27655 (D.A.P.) and the UC Berkeley Tang Distinguished Scholarship (Y.Z.).

REFERENCES

- Freitag NE, Port GC, Miner MD. 2009. *Listeria monocytogenes*—from saprophyte to intracellular pathogen. *Nat Rev Microbiol* 7:623–628. <https://doi.org/10.1038/nrmicro2171>.
- Radosheвич L, Cossart P. 2018. *Listeria monocytogenes*: towards a complete picture of its physiology and pathogenesis. *Nat Rev Microbiol* 16:32–46. <https://doi.org/10.1038/nrmicro.2017.126>.
- Scotti M, Monzo HJ, Lacharme-Lora L, Lewis DA, Vazquez-Boland JA. 2007. The PrfA virulence regulon. *Microbes Infect* 9:1196–1207. <https://doi.org/10.1016/j.micinf.2007.05.007>.
- Pizarro-Cerda J, Cossart P. 2006. Subversion of cellular functions by *Listeria monocytogenes*. *J Pathol* 208:215–223. <https://doi.org/10.1002/path.1888>.
- Mitchell G, Cheng MI, Chen C, Nguyen BN, Whiteley AT, Kianian S, Cox JS, Green DR, McDonald KL, Portnoy DA. 2018. *Listeria monocytogenes* triggers noncanonical autophagy upon phagocytosis, but avoids subsequent growth-restricting xenophagy. *Proc Natl Acad Sci U S A* 115:E210–E217. <https://doi.org/10.1073/pnas.1716055115>.
- Reniere ML, Whiteley AT, Hamilton KL, John SM, Lauer P, Brennan RG, Portnoy DA. 2015. Glutathione activates virulence gene expression of an intracellular pathogen. *Nature* 517:170–173. <https://doi.org/10.1038/nature14029>.
- Anaya-Sanchez A, Feng Y, Berude JC, Portnoy DA. 2021. Detoxification of methylglyoxal by the glyoxalase system is required for glutathione availability and virulence activation in *Listeria monocytogenes*. *PLoS Pathog* 17:e1009819. <https://doi.org/10.1371/journal.ppat.1009819>.

8. Rivera-Lugo R, Light SH, Garelis NE, Portnoy DA. 2022. RibU is an essential determinant of *Listeria* pathogenesis that mediates acquisition of FMN and FAD during intracellular growth. *Proc Natl Acad Sci U S A* 119:e2122173119. <https://doi.org/10.1073/pnas.2122173119>.
9. Masters PA, O'Bryan TA, Zurlo J, Miller DQ, Joshi N. 2003. Trimethoprim-sulfamethoxazole revisited. *Arch Intern Med* 163:402–410. <https://doi.org/10.1001/archinte.163.4.402>.
10. Ducker GS, Rabinowitz JD. 2017. One-carbon metabolism in health and disease. *Cell Metab* 25:27–42. <https://doi.org/10.1016/j.cmet.2016.08.009>.
11. Nichols BP, Seibold AM, Doktor SZ. 1989. *para*-Aminobenzoate synthesis from chorismate occurs in two steps. *J Biol Chem* 264:8597–8601. [https://doi.org/10.1016/S0021-9258\(18\)81833-6](https://doi.org/10.1016/S0021-9258(18)81833-6).
12. Ye QZ, Liu J, Walsh CT. 1990. *p*-Aminobenzoate synthesis in *Escherichia coli*: purification and characterization of PabB as aminodeoxychorismate synthase and enzyme X as aminodeoxychorismate lyase. *Proc Natl Acad Sci U S A* 87:9391–9395. <https://doi.org/10.1073/pnas.87.23.9391>.
13. Green JM, Nichols BP. 1991. *p*-Aminobenzoate biosynthesis in *Escherichia coli*. Purification of aminodeoxychorismate lyase and cloning of pabC. *J Biol Chem* 266:12971–12975. [https://doi.org/10.1016/S0021-9258\(18\)98790-9](https://doi.org/10.1016/S0021-9258(18)98790-9).
14. Green JM, Merkel WK, Nichols BP. 1992. Characterization and sequence of *Escherichia coli* pabC, the gene encoding aminodeoxychorismate lyase, a pyridoxal phosphate-containing enzyme. *J Bacteriol* 174:5317–5323. <https://doi.org/10.1128/jb.174.16.5317-5323.1992>.
15. Roux B, Walsh CT. 1992. *p*-Aminobenzoate synthesis in *Escherichia coli*: kinetic and mechanistic characterization of the amidotransferase PabA. *Biochemistry* 31:6904–6910. <https://doi.org/10.1021/bi00145a006>.
16. Viswanathan VK, Green JM, Nichols BP. 1995. Kinetic characterization of 4-amino 4-deoxychorismate synthase from *Escherichia coli*. *J Bacteriol* 177:5918–5923. <https://doi.org/10.1128/jb.177.20.5918-5923.1995>.
17. Rayl EA, Green JM, Nichols BP. 1996. *Escherichia coli* aminodeoxychorismate synthase: analysis of pabB mutations affecting catalysis and subunit association. *Biochim Biophys Acta* 1295:81–88. [https://doi.org/10.1016/0167-4838\(96\)00029-5](https://doi.org/10.1016/0167-4838(96)00029-5).
18. Anderson KS, Kati WM, Ye QZ, Liu J, Walsh CT, Benesi AJ, Johnson KA. 1991. Isolation and structure elucidation of the 4-amino-4-deoxychorismate intermediate in the PABA enzymic pathway. *J Am Chem Soc* 113:3198–3200. <https://doi.org/10.1021/ja00008a073>.
19. Slock J, Stahly DP, Han CY, Six EW, Crawford IP. 1990. An apparent *Bacillus subtilis* folic acid biosynthetic operon containing pab, an amphibolic trpG gene, a third gene required for synthesis of para-aminobenzoic acid, and the dihydropteroate synthase gene. *J Bacteriol* 172:7211–7226. <https://doi.org/10.1128/jb.172.12.7211-7226.1990>.
20. Shuvalov O, Petukhov A, Daks A, Fedorova O, Vasileva E, Barlev NA. 2017. One-carbon metabolism and nucleotide biosynthesis as attractive targets for anticancer therapy. *Oncotarget* 8:23955–23977. <https://doi.org/10.18632/oncotarget.15053>.
21. Marquis H, Bouwer HG, Hinrichs DJ, Portnoy DA. 1993. Intracytoplasmic growth and virulence of *Listeria monocytogenes* auxotrophic mutants. *Infect Immun* 61:3756–3760. <https://doi.org/10.1128/iai.61.9.3756-3760.1993>.
22. Pistor S, Chakraborty T, Niebuhr K, Domann E, Wehland J. 1994. The ActA protein of *Listeria monocytogenes* acts as a nucleator inducing reorganization of the actin cytoskeleton. *EMBO J* 13:758–763. <https://doi.org/10.1002/j.1460-2075.1994.tb06318.x>.
23. Niebuhr K, Chakraborty T, Rohde M, Gazlig T, Jansen B, Kollner P, Wehland J. 1993. Localization of the ActA polypeptide of *Listeria monocytogenes* in infected tissue culture cell lines: ActA is not associated with actin “comets.” *Infect Immun* 61:2793–2802. <https://doi.org/10.1128/iai.61.7.2793-2802.1993>.
24. Skoble J, Portnoy DA, Welch MD. 2000. Three regions within ActA promote Arp2/3 complex-mediated actin nucleation and *Listeria monocytogenes* motility. *J Cell Biol* 150:527–538. <https://doi.org/10.1083/jcb.150.3.527>.
25. Cheng MI, Chen C, Engstrom P, Portnoy DA, Mitchell G. 2018. Actin-based motility allows *Listeria monocytogenes* to avoid autophagy in the macrophage cytosol. *Cell Microbiol* 20:e12854. <https://doi.org/10.1111/cmi.12854>.
26. Tran PV, Nichols BP. 1991. Expression of *Escherichia coli* pabA. *J Bacteriol* 173:3680–3687. <https://doi.org/10.1128/jb.173.12.3680-3687.1991>.
27. Carter EL, Jager L, Gardner L, Hall CC, Willis S, Green JM. 2007. *Escherichia coli* abg genes enable uptake and cleavage of the folate catabolite *p*-aminobenzoyl-glutamate. *J Bacteriol* 189:3329–3334. <https://doi.org/10.1128/JB.01940-06>.
28. Hussein MJ, Green JM, Nichols BP. 1998. Characterization of mutations that allow *p*-aminobenzoyl-glutamate utilization by *Escherichia coli*. *J Bacteriol* 180:6260–6268. <https://doi.org/10.1128/JB.180.23.6260-6268.1998>.
29. Shane B, Stokstad EL. 1975. Transport and metabolism of folates by bacteria. *J Biol Chem* 250:2243–2253. [https://doi.org/10.1016/S0021-9258\(19\)41709-2](https://doi.org/10.1016/S0021-9258(19)41709-2).
30. Ronneau S, Hallez R. 2019. Make and break the alarmone: regulation of (p)ppGpp synthetase/hydrolase enzymes in bacteria. *FEMS Microbiol Rev* 43:389–400. <https://doi.org/10.1093/femsre/fuz009>.
31. Mechold U, Cashel M, Steiner K, Gentry D, Malke H. 1996. Functional analysis of a *relA*/spoT gene homolog from *Streptococcus equisimilis*. *J Bacteriol* 178:1401–1411. <https://doi.org/10.1128/jb.178.5.1401-1411.1996>.
32. Geiger T, Kastle B, Gratani FL, Goerke C, Wolz C. 2014. Two small (p)ppGpp synthetases in *Staphylococcus aureus* mediate tolerance against cell envelope stress conditions. *J Bacteriol* 196:894–902. <https://doi.org/10.1128/JB.01201-13>.
33. Lemos JA, Lin VK, Nascimento MM, Abranches J, Burne RA. 2007. Three gene products govern (p)ppGpp production by *Streptococcus mutans*. *Mol Microbiol* 65:1568–1581. <https://doi.org/10.1111/j.1365-2958.2007.05897.x>.
34. Nanamiya H, Kasai K, Nozawa A, Yun CS, Narisawa T, Murakami K, Natori Y, Kawamura F, Tozawa Y. 2008. Identification and functional analysis of novel (p)ppGpp synthetase genes in *Bacillus subtilis*. *Mol Microbiol* 67:291–304. <https://doi.org/10.1111/j.1365-2958.2007.06018.x>.
35. Whiteley AT, Pollock AJ, Portnoy DA. 2015. The PAMP c-di-AMP is essential for *Listeria monocytogenes* growth in rich but not minimal media due to a toxic increase in (p)ppGpp. *Cell Host Microbe* 17:788–798. <https://doi.org/10.1016/j.chom.2015.05.006>. (Erratum, 18:132, 10.1016/j.chom.2015.06.005.)
36. Goncharoff P, Nichols BP. 1988. Evolution of aminobenzoate synthetases: nucleotide sequences of *Salmonella typhimurium* and *Klebsiella aerogenes* pabB. *Mol Biol Evol* 5:531–548. <https://doi.org/10.1093/oxfordjournals.molbev.a040512>.
37. Kaplan JB, Merkel WK, Nichols BP. 1985. Evolution of glutamine amidotransferase genes. Nucleotide sequences of the pabA genes from *Salmonella typhimurium*, *Klebsiella aerogenes* and *Serratia marcescens*. *J Mol Biol* 183:327–340. [https://doi.org/10.1016/0022-2836\(85\)90004-x](https://doi.org/10.1016/0022-2836(85)90004-x).
38. Gazzali AM, Lobry M, Colombeau L, Acherar S, Azais H, Mordon S, Arnoux P, Baros F, Vanderesse R, Frochot C. 2016. Stability of folic acid under several parameters. *Eur J Pharm Sci* 93:419–430. <https://doi.org/10.1016/j.ejps.2016.08.045>.
39. Liang L. 2020. Folates: stability and interaction with biological molecules. *J Agric Food Res* 2:100039. <https://doi.org/10.1016/j.jafr.2020.100039>.
40. Zheng Y, Cantley LC. 2019. Toward a better understanding of folate metabolism in health and disease. *J Exp Med* 216:253–266. <https://doi.org/10.1084/jem.20181965>.
41. Leimeister-Wachter M, Haffner C, Domann E, Goebel W, Chakraborty T. 1990. Identification of a gene that positively regulates expression of listeriolysin, the major virulence factor of *Listeria monocytogenes*. *Proc Natl Acad Sci U S A* 87:8336–8340. <https://doi.org/10.1073/pnas.87.21.8336>.
42. Kref J, Vazquez-Boland JA. 2001. Regulation of virulence genes in *Listeria*. *Int J Med Microbiol* 291:145–157. <https://doi.org/10.1078/1438-4221-00111>.
43. Leimeister-Wachter M, Domann E, Chakraborty T. 1991. Detection of a gene encoding a phosphatidylinositol-specific phospholipase C that is co-ordinately expressed with listeriolysin in *Listeria monocytogenes*. *Mol Microbiol* 5:361–366. <https://doi.org/10.1111/j.1365-2958.1991.tb02117.x>.
44. Vazquez-Boland JA, Kocks C, Dramsi S, Ohayon H, Geoffroy C, Mengaud J, Cossart P. 1992. Nucleotide sequence of the lecithinase operon of *Listeria monocytogenes* and possible role of lecithinase in cell-to-cell spread. *Infect Immun* 60:219–230. <https://doi.org/10.1128/iai.60.1.219-230.1992>.
45. Poyart C, Abachin E, Razafimanantsoa I, Berche P. 1993. The zinc metalloprotease of *Listeria monocytogenes* is required for maturation of phosphatidylcholine phospholipase C: direct evidence obtained by gene complementation. *Infect Immun* 61:1576–1580. <https://doi.org/10.1128/iai.61.4.1576-1580.1993>.
46. Kocks C, Gouin E, Tabouret M, Berche P, Ohayon H, Cossart P. 1992. L. monocytogenes-induced actin assembly requires the actA gene product, a surface protein. *Cell* 68:521–531. [https://doi.org/10.1016/0092-8674\(92\)90188-i](https://doi.org/10.1016/0092-8674(92)90188-i).
47. Pizarro-Cerda J, Kuhbacher A, Cossart P. 2012. Entry of *Listeria monocytogenes* in mammalian epithelial cells: an updated view. *Cold Spring Harb Perspect Med* 2:a010009. <https://doi.org/10.1101/cshperspect.a010009>.
48. Dussurget O, Cabanes D, Dehoux P, Lecuit M, Buchrieser C, Glaser P, Cossart P, European *Listeria* Genome Consortium. 2002. *Listeria monocytogenes* bile salt hydrolase is a PrfA-regulated virulence factor involved in the intestinal and hepatic phases of listeriosis. *Mol Microbiol* 45:1095–1106. <https://doi.org/10.1046/j.1365-2958.2002.03080.x>.

49. Mengaud J, Dramsi S, Gouin E, Vazquez-Boland JA, Milon G, Cossart P. 1991. Pleiotropic control of *Listeria monocytogenes* virulence factors by a gene that is autoregulated. *Mol Microbiol* 5:2273–2283. <https://doi.org/10.1111/j.1365-2958.1991.tb02158.x>.
50. Chakraborty T, Leimeister-Wachter M, Domann E, Hartl M, Goebel W, Nichterlein T, Notermans S. 1992. Coordinate regulation of virulence genes in *Listeria monocytogenes* requires the product of the *prfA* gene. *J Bacteriol* 174:568–574. <https://doi.org/10.1128/jb.174.2.568-574.1992>.
51. Ripio MT, Dominguez-Bernal G, Lara M, Suarez M, Vazquez-Boland JA. 1997. A Gly145Ser substitution in the transcriptional activator PrfA causes constitutive overexpression of virulence factors in *Listeria monocytogenes*. *J Bacteriol* 179:1533–1540. <https://doi.org/10.1128/jb.179.5.1533-1540.1997>.
52. Vega Y, Dickneite C, Ripio MT, Bockmann R, Gonzalez-Zorn B, Novella S, Dominguez-Bernal G, Goebel W, Vazquez-Boland JA. 1998. Functional similarities between the *Listeria monocytogenes* virulence regulator PrfA and cyclic AMP receptor protein: the PrfA* (Gly145Ser) mutation increases binding affinity for target DNA. *J Bacteriol* 180:6655–6660. <https://doi.org/10.1128/JB.180.24.6655-6660.1998>.
53. Lobel L, Sigal N, Borovok I, Belitsky BR, Sonenshein AL, Herskovits AA. 2015. The metabolic regulator CodY links *Listeria monocytogenes* metabolism to virulence by directly activating the virulence regulatory gene *prfA*. *Mol Microbiol* 95:624–644. <https://doi.org/10.1111/mmi.12890>.
54. Lobel L, Sigal N, Borovok I, Ruppin E, Herskovits AA. 2012. Integrative genomic analysis identifies isoleucine and CodY as regulators of *Listeria monocytogenes* virulence. *PLoS Genet* 8:e1002887. <https://doi.org/10.1371/journal.pgen.1002887>.
55. Janeway CA, Jr. 1989. Approaching the asymptote? Evolution and revolution in immunology. *Cold Spring Harbor Symp Quant Biol* 54(Part 1):1–13. <https://doi.org/10.1101/sqb.1989.054.01.003>.
56. Janeway CA, Jr, Medzhitov R. 2002. Innate immune recognition. *Annu Rev Immunol* 20:197–216. <https://doi.org/10.1146/annurev.immunol.20.083001.084359>.
57. Kumar H, Kawai T, Akira S. 2011. Pathogen recognition by the innate immune system. *Int Rev Immunol* 30:16–34. <https://doi.org/10.3109/08830185.2010.529976>.
58. Akberova SI, Tazulakhova EB, Musaev-Galbinur PI, Leont'eva NA, Stroeva OG. 1999. Para-aminobenzoic acid—an interferon inducer. *Antibiot Khimioter* 44:17–20. (In Russian.)
59. Akberova SI. 2002. New biological properties of p-aminobenzoic acid Izv Akad Nauk Ser Biol 2002:477–481. (In Russian.)
60. Alam SS, Nambudiri AM, Rudney H. 1975. 4-Hydroxybenzoate:polyprenyl transferase and the prenylation of 4-aminobenzoate in mammalian tissues. *Arch Biochem Biophys* 171:183–190. [https://doi.org/10.1016/0003-9861\(75\)90022-3](https://doi.org/10.1016/0003-9861(75)90022-3).
61. Gonzalez-Aragon D, Buron MI, Lopez-Lluch G, Herman MD, Gomez-Diaz C, Navas P, Villalba JM. 2005. Coenzyme Q and the regulation of intracellular steady-state levels of superoxide in HL-60 cells. *Biofactors* 25:31–41. <https://doi.org/10.1002/biof.5520250105>.
62. Simon R, Priefer U, Pühler A. 1983. A broad host range mobilization system for in vivo genetic engineering: transposon mutagenesis in Gram negative bacteria. *Nat Biotechnol* 1:784–791. <https://doi.org/10.1038/nbt1183-784>.
63. Lauer P, Chow MY, Loessner MJ, Portnoy DA, Calendar R. 2002. Construction, characterization, and use of two *Listeria monocytogenes* site-specific phage integration vectors. *J Bacteriol* 184:4177–4186. <https://doi.org/10.1128/JB.184.15.4177-4186.2002>.
64. Camilli A, Tilney LG, Portnoy DA. 1993. Dual roles of *plcA* in *Listeria monocytogenes* pathogenesis. *Mol Microbiol* 8:143–157. <https://doi.org/10.1111/j.1365-2958.1993.tb01211.x>.
65. National Research Council. 2011. Guide for the care and use of laboratory animals, 8th ed. National Academies Press, Washington, DC.
66. Sun AN, Camilli A, Portnoy DA. 1990. Isolation of *Listeria monocytogenes* small-plaque mutants defective for intracellular growth and cell-to-cell spread. *Infect Immun* 58:3770–3778. <https://doi.org/10.1128/iai.58.11.3770-3778.1990>.
67. Zemansky J, Kline BC, Woodward JJ, Leber JH, Marquis H, Portnoy DA. 2009. Development of a mariner-based transposon and identification of *Listeria monocytogenes* determinants, including the peptidyl-prolyl isomerase PrsA2, that contribute to its hemolytic phenotype. *J Bacteriol* 191:3950–3964. <https://doi.org/10.1128/JB.00016-09>.
68. Becavin C, Bouchier C, Lechat P, Archambaud C, Creno S, Gouin E, Wu Z, Kuhbacher A, Brisse S, Pucciarelli MG, Garcia-del Portillo F, Hain T, Portnoy DA, Chakraborty T, Lecuit M, Pizarro-Cerda J, Moszer I, Bierne H, Cossart P. 2014. Comparison of widely used *Listeria monocytogenes* strains EGD, 10403S, and EGD-e highlights genomic variations underlying differences in pathogenicity. *mBio* 5:e00969-14. <https://doi.org/10.1128/mBio.00969-14>.
69. Miner MD, Port GC, Freitag NE. 2008. Functional impact of mutational activation on the *Listeria monocytogenes* central virulence regulator PrfA. *Microbiology (Reading)* 154:3579–3589. <https://doi.org/10.1099/mic.0.2008/021063-0>.